

Radio Vortex Wireless Communications With Non-Coaxial UCA Transceiver

Haiyue Jing and Wenchi Cheng

State Key Laboratory of Integrated Services Networks, Xidian University, Xi'an, China

E-mail: {hyjing@stu.xidian.edu.cn, wccheng@xidian.edu.cn}

Abstract—In the past decade, more and more researchers have concentrated on orbital-angular-momentum (OAM) based radio vortex wireless communications, which is expected to provide orthogonality among different OAM-modes. The uniform circular array (UCA) is considered as one promising antenna structure for OAM based radio vortex wireless communications. However, most studies regarding UCA focus on the scenario where the transmit and receive UCAs are aligned with each other. In this paper, we investigate the radio vortex wireless communications with non-coaxial UCA, i.e., the UCA transceivers are parallel but non-coaxial. We study the channel model and develop the mode-decomposition scheme to decompose the OAM-modes. Then, we discuss the impact of included angles on the channel model under non-coaxial scenario. Numerical results are presented to evaluate our developed scheme and show that the spectrum efficiency of the non-coaxial UCA transceiver in some cases is larger than that of the aligned UCA transceiver based radio vortex wireless communications.

Index Terms—Orbital angular momentum (OAM), uniform circular array (UCA), non-coaxial UCA, radio vortex wireless communications.

I. INTRODUCTION

THE plane wave based wireless communications have becoming more and more matured, along with the well utilization of the traditional resources such as time and frequency [1]. To further increase the spectrum efficiency, an efficient way is to explore other dimensional resources. During the past decade, orbital-angular-momentum (OAM), which is a kind of wavefront with helical phase front, has been attracted much attentions because different OAM-modes and the OAM-modes are orthogonal with each other [2]–[4]. Thus, using multiple OAM-modes for information transmission are expected to increase the spectrum efficiency for wireless communications.

So far, many researches and experiments have been conducted to verify the feasibility of OAM based radio vortex wireless communications. The authors of [3] demonstrated a 32 Gbps millimeter-wave link using four OAM-modes on each of two polarizations for data transmission. The authors of [5] experimentally demonstrated a 60 GHz wireless communications link using two OAM-modes. The authors of [6] theoretically and experimentally concluded that mode division multiplexing using OAM can reduce the receiver complexity and achieve high spectrum efficiency. In addition,

the authors of [7], [8] held that OAM can be used in future wireless broadband communications because of its potential ability to achieve high spectrum efficiency. Apart from the radio vortex wireless communications, OAM based free-space optical communications has also been extensively studied [9], [10].

Specifically, uniform circular array (UCA) based OAM is considered as one promising antenna architecture for radio vortex wireless communications because of its flexibility in transmitting multiple OAM beams with different OAM-modes [11], [12]. The schemes of OAM with index modulation were proposed to achieve much better error performance than the OAM based mode division multiplexing schemes [13]. The authors of [14] proposed a mode-hopping scheme within the narrow frequency band for anti-jamming in wireless communications, which can achieve the same anti-jamming results as compared with the conventional wideband frequency-hopping schemes. The authors of [15] proposed concentric UCAs system where the transmit and receive UCAs are aligned with each other to increase the spectrum efficiency.

For the UCA antenna structure, it is now highly demanded for strict alignment between the transmit and receive UCAs in current researches. However, for wireless communications, it is not practical to maintain the transceiver aligned with each other. If the transmit and receive UCAs are non-coaxial with each other, the phase of received signal contains not only the phase of OAM-mode, but also the phase turbulence due to unequal distance transmission at different places of the receiver [16], which challenges the efficient receiving for radio vortex wireless communications. Thus, a question is raised that how to decompose the OAM beams with multiple OAM-modes when the transmit and receive UCAs are non-coaxial.

To overcome the above-mentioned problem, in this paper we derive the mathematical model to characterize channel of non-coaxial radio vortex wireless communications. Based on the channel model, we develop the mode-decomposition scheme to obtain the signal corresponding to each OAM-mode. Also, the impact of concluded angles on the channel model is discussed. We conduct extensive simulations to validate and evaluate that the spectrum efficiency of the non-coaxial UCA transceiver under some non-coaxial cases is larger than that of the aligned UCA transceiver in radio vortex wireless communications.

The rest of this paper is organized as follows. Section II

This work was supported in part by the National Natural Science Foundation of China (No. 61771368) and the Young Elite Scientists Sponsorship Program by CAST (2016QNRC001).

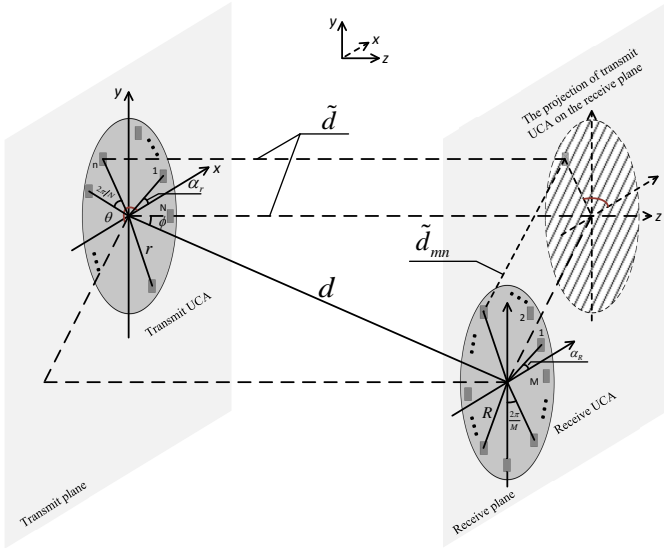


Fig. 1. The system model for the non-coaxial UCA transceiver based radio vortex wireless communications.

gives the non-coaxial UCA transceiver based radio vortex wireless communications model. Section III investigates the channel model and develops the mode-decomposition scheme to obtain the receive signal corresponding to each OAM-mode. Section IV evaluates our developed scheme and discusses the channel amplitude gains versus the included angles under non-coaxial scenario. The paper concludes with Section V.

II. THE NON-COAXIAL UCAS BASED SYSTEM MODEL FOR RADIO VORTEX WIRELESS COMMUNICATION

Figure 1 depicts the system model for the non-coaxial UCA transceiver based radio vortex wireless communications, where the transmit and receive UCAs are non-coaxial and the size of them can be different. The planes corresponding to the transmit and the receive UCAs are the transmit plane and the receive plane, respectively. The projection of the transmit UCA is on the receive plane. We denoted by d the distance from the center of the transmit UCA to the center of the receive UCA. The transmit and receive UCAs are equipped with N array-elements and M array-elements, respectively. For the transmit UCA, the array-elements, which are fed with the same input signal but with a successive delay from array-element to array-element such that after a full turn the phase has been incremented by an integer multiple l of 2π , are uniformly around the perimeter of the circle and l represents the number of topological charges, i.e., the number of OAM-modes. For the receive UCA, the array-elements are also uniformly around perimeter of the circle. We denote by α_r and α_R the angles between the phase angle of the first array-element and zero radian corresponding to the transmit and receive UCAs, respectively. The parameter θ denotes the included angle between x -axis and the projection of the line from the center of the transmit UCA to the center of the receive UCA on the transmit plane. Also, ϕ denotes

the included angle between z -axis and the line from the center of the transmit UCA to the center of the receive UCA. The notation \tilde{d} represents the distance between the center of the transmit UCA and the center of the receive UCA. The parameter \tilde{d}_{mn} is the distance between the projection of the n th ($1 \leq n \leq N$) transmit array-element on the receive plane and the m th ($1 \leq m \leq M$) receive array-element. We also denote by r the radius of transmit UCA and R the radius of receive UCA. In the following, we derive the channel model and develop the mode-decomposition scheme to obtain the signal corresponding to each OAM-mode.

III. CHANNEL MODEL AND THE MODE-DECOMPOSITION SCHEME FOR NON-COAXIAL UCAS BASED RADIO VORTEX WIRELESS COMMUNICATIONS

The signal at the n th array-element on the transmit UCA, denoted by x_n , is given as follows:

$$\begin{aligned} x_n &= \sum_{l=\lfloor \frac{2-N}{2} \rfloor}^{\lfloor N/2 \rfloor} \frac{1}{\sqrt{N}} s_l e^{j(\varphi_n + \alpha_r)l} \\ &= \sum_{l=\lfloor \frac{2-N}{2} \rfloor}^{\lfloor N/2 \rfloor} \frac{1}{\sqrt{N}} s_l e^{j[\frac{2\pi(n-1)}{N} + \alpha_r]l}, \end{aligned} \quad (1)$$

where $(\varphi_n + \alpha_r)$ is the azimuthal angle, defined as the angular position on a plane perpendicular to the axis of propagation, corresponding to the n th array-element on the transmit UCA. $\varphi_n = 2\pi(n-1)/N$ is the basic angle for the transmit UCA. The symbol s_l denotes the signal on the l th OAM-mode of the transmit UCA. $l \in [\lfloor (2-N)/2 \rfloor, \lfloor N/2 \rfloor]$ is the OAM-mode number. When $\kappa < 0$, $\lfloor \kappa \rfloor$ represents the smallest integer which is greater than or equal to κ . When $\kappa \geq 0$, $\lfloor \kappa \rfloor$ represents the largest integer which is less than or equal to κ .

We denote by h_{mn} the channel gain from the n th array-element on the transmit UCA to the m th array-element on the receive UCA. Then, h_{mn} can be written as follows [17]:

$$h_{mn} = \frac{\beta \lambda e^{-j\frac{2\pi}{\lambda} d_{mn}}}{4\pi d_{mn}}, \quad (2)$$

where β denotes the combination of all the relevant constants such as attenuation and phase rotation caused by antennas and their patterns on both sides. The parameter d_{mn} is the distance between the n th array-element on the transmit UCA and the m th array-element on the receive UCA. We denote by \tilde{d}_{mn} the distance between the projection of the n th array-element on the transmit UCA in the receive plane and the m th array-element on the receive UCA. Since the transmit UCA and the projection of transmit UCA are aligned well with each other, the distance \tilde{d}_{mn} should be derived first if we want to obtain d_{mn} .

In terms of rectangular coordinates, the coordinate of the n th array-element on the transmit UCA is $(r \cos(\varphi_n + \alpha_r), r \sin(\varphi_n + \alpha_r), 0)$. The coordinate corresponding to the center of the receive UCA is $(d \sin \phi \cos \theta, d \sin \phi \sin \theta, d \cos \phi)$. Then, we have $\tilde{d} = d \cos \phi$. Thus, the coordinate related to the projection

$$\begin{aligned}\tilde{d}_{mn} &= \sqrt{[R \cos(\psi_m + a_R) - d \sin \phi \cos \theta - r \cos(\varphi_n + \alpha_r)]^2 + [R \sin(\psi_m + a_R) - d \sin \phi \sin \theta - r \sin(\varphi_n + \alpha_r)]^2} \\ &= \sqrt{R^2 + r^2 + d^2 \sin^2 \phi - 2rR \cos(\psi_m + a_R - \varphi_n - \alpha_r) - 2Rd \sin \phi \cos(\psi_m + a_R - \theta) + 2rd \sin \phi \cos(\varphi_n + \alpha_r - \theta)}.\end{aligned}\quad (3)$$

$$\begin{aligned}d_{mn} &= \sqrt{\tilde{d}_{mn}^2 + \tilde{d}^2} \\ &= \sqrt{R^2 + r^2 + d^2 - 2rR \cos(\psi_m + a_R - \varphi_n - \alpha_r) - 2Rd \sin \phi \cos(\psi_m + a_R - \theta) + 2rd \sin \phi \cos(\varphi_n + \alpha_r - \theta)} \\ &= \sqrt{R^2 + r^2 + d^2} \sqrt{1 - \frac{2rR \cos(\psi_m + a_R - \varphi_n - \alpha_r) + 2Rd \sin \phi \cos(\psi_m + a_R - \theta) - 2rd \sin \phi \cos(\varphi_n + \alpha_r - \theta)}{R^2 + r^2 + d^2}} \\ &\approx \sqrt{R^2 + r^2 + d^2} - \frac{rR \cos(\psi_m + a_R - \varphi_n - \alpha_r) + Rd \sin \phi \cos(\psi_m + a_R - \theta) - rd \sin \phi \cos(\varphi_n + \alpha_r - \theta)}{\sqrt{R^2 + r^2 + d^2}}.\end{aligned}\quad (4)$$

$$\begin{aligned}h_{mn} &= \underbrace{\frac{\beta \lambda}{4\pi \sqrt{d^2 + r^2 + R^2}} \exp\left(\frac{-j2\pi \sqrt{d^2 + r^2 + R^2}}{\lambda}\right) \exp\left[\frac{j2\pi Rd \sin \phi \cos(\psi_m + a_R - \theta)}{\lambda \sqrt{d^2 + r^2 + R^2}}\right]}_{A_m} \\ &\quad \times \exp\left[-j \underbrace{\frac{2\pi r \sqrt{R^2 + d^2 \sin^2 \phi - 2Rd \sin \phi \cos(\psi_m + a_R - \theta)}}{\lambda \sqrt{d^2 + r^2 + R^2}}}_{B_m} \sin(\varphi_n + \alpha_r - \psi_m - a_R + \zeta_m)\right].\end{aligned}\quad (7)$$

of the n th array-element on the transmit UCA in the receive plane is $(r \cos(\varphi_n + \alpha_r), r \sin(\varphi_n + \alpha_r), d \cos \phi)$ and the coordinate of the m th array-element on the receive UCA is $(R \cos(\psi_m + a_R) - d \sin \phi \cos \theta, R \sin(\psi_m + a_R) - d \sin \phi \sin \theta, d \cos \phi)$. Similar to the azimuthal angle at the transmit UCA, $\psi_m + a_R$ is the azimuthal angle of the m th array-element on the receive UCA and $\psi_m = 2\pi(m-1)/M$ is the basic angle for the receive UCA. Therefore, \tilde{d}_{mn} is derived in Eq. (3).

Then, using the Pythagorean theorem we can derived d_{mn} in Eq. (4). Because $d \gg R$ and $d \gg r$, we have $d_{mn} \approx \sqrt{d^2 + R^2 + r^2}$ for the denominator in Eq. (2). For d_{mn} in the numerator, which is part of the item $\exp(-j2\pi d_{mn}/\lambda)$, we can approximate it using $\sqrt{1-2x} \approx 1-x$ when x is very close to zero as shown in Eq. (4).

In Eq. (4), the item $[2rR \cos(\psi_m + a_R - \varphi_n - \alpha_r) - 2rd \sin \phi \cos(\varphi_n + \alpha_r - \theta)]$ can be derived as follows:

$$\begin{aligned}&rR \cos(\psi_m + a_R - \varphi_n - \alpha_r) - rd \sin \phi \cos(\varphi_n + \alpha_r - \theta) \\ &= [Rr - rd \sin \phi \cos(\psi_m + a_R - \theta)] \cos(\varphi_n + \alpha_r - \psi_m - a_R) \\ &\quad + rd \sin \phi \sin(\psi_m + a_R - \theta) \sin(\varphi_n + \alpha_r - \psi_m - a_R) \\ &= r \sqrt{R^2 + d^2 \sin^2 \phi - 2Rd \sin \phi \cos(\psi_m + a_R - \theta)} \\ &\quad \times \sin(\varphi_n + \alpha_r - \psi_m - a_R + \zeta_m),\end{aligned}\quad (5)$$

where

$$\begin{cases} \sin \zeta_m = \frac{R - d \sin \phi \cos(\psi_m + a_R - \theta)}{\sqrt{R^2 + d^2 \sin^2 \phi - 2Rd \sin \phi \cos(\psi_m + a_R - \theta)}}; \\ \cos \zeta_m = \frac{d \sin \phi \sin(\psi_m + a_R - \theta)}{\sqrt{R^2 + d^2 \sin^2 \phi - 2Rd \sin \phi \cos(\psi_m + a_R - \theta)}}.\end{cases}\quad (6)$$

Associating Eqs. (2), (4), (5), and (6), the channel gain h_{mn} can be derived as Eq. (7). For convenient expression, we replace some polynomials in Eq. (7) with A_m and B_m , respectively, as shown in Eq. (7).

The received signal at the m th array-element, denoted by y_m , can be derived as follows:

$$\begin{aligned}y_m &= \sum_{n=1}^N \sum_{l=\lfloor \frac{2-N}{2} \rfloor}^{\lfloor N/2 \rfloor} h_{mn} \frac{1}{\sqrt{N}} s_l e^{j \frac{2\pi(n-1)l}{N}} + z_m \\ &= \sum_{l=\lfloor \frac{2-N}{2} \rfloor}^{\lfloor N/2 \rfloor} \tilde{h}_{ml} s_l + z_m,\end{aligned}\quad (8)$$

where z_m denotes the received noise at the m th array-element on the receive UCA and z_m is complex Gaussian variable with zero mean and variance σ_m^2 . We denote by \tilde{h}_{ml} the channel gain from the transmit UCA to the m th array-element on the receive UCA corresponding to the l th OAM-mode. The channel gain \tilde{h}_{ml} is given by Eq. (9). In Eq. (9), φ is the continuous variable related to φ_n ranging from 0 and 2π . When n is equal to 1, φ_n is equal to zero. When $n = N$, φ_n is equal to $2\pi - 2\pi/N$ and very close to 2π . To express conveniently, we denote by $\psi = \alpha_r - \psi_m - a_R + \zeta_m$, which is used in Eq. (9).

$$\begin{aligned}
\tilde{h}_{ml} &= \sum_{n=1}^N \frac{1}{\sqrt{N}} h_{mn} e^{j\frac{2\pi(n-1)}{N}l} = \sum_{n=1}^N \frac{A_m}{\sqrt{N}} \exp[-B_m \sin(\varphi_n + \alpha_r - \psi_m - a_R + \zeta_m)] \exp[j(\varphi_n + \alpha_r)l] \\
&= \frac{A_m}{\sqrt{N}} \exp[j(\psi_m + a_R - \zeta_m)l] \sum_{n=1}^N \exp[j(\varphi_n + \alpha_r - \psi_m - a_R + \zeta_m)l] \exp[-B_m \sin(\varphi_n + \alpha_r - \psi_m - a_R + \zeta_m)] \\
&\approx \sqrt{N} A_m \exp[j(\psi_m + a_R - \zeta_m)l] \frac{1}{2\pi} \int_0^{2\pi} \exp[j(\varphi + \underbrace{\alpha_r - \psi_m - a_R + \zeta_m}_{\psi})l] \exp[-B_m \sin(\varphi + \alpha_r - \psi_m - a_R + \zeta_m)] d\varphi \\
&= \sqrt{N} A_m \exp[j(\psi_m + a_R - \zeta_m)l] \frac{1}{2\pi} \int_{\psi}^{2\pi+\psi} \exp[j(\varphi + \psi)l] \exp[-B_m \sin(\varphi + \psi)] d(\varphi + \psi) \\
&= \sqrt{N} A_m \exp[j(\psi_m + a_R - \zeta_m)l] \frac{1}{2\pi} \int_0^{2\pi} \exp[j(\varphi + \psi)l] \exp[-B_m \sin(\varphi + \psi)] d(\varphi + \psi) \\
&= \sqrt{N} A_m \exp[j(\psi_m + a_R - \zeta_m)l] J_l(B_m) \\
&= \underbrace{\frac{\sqrt{N}\beta\lambda}{4\pi\sqrt{d^2 + r^2 + R^2}} \exp\left(\frac{-j2\pi\sqrt{d^2 + r^2 + R^2}}{\lambda}\right)}_h \exp[j(\psi_m + a_R - \zeta_m)l] \\
&\quad \times \underbrace{\exp\left[\frac{j2\pi R d \sin\phi \cos(\psi_m + a_R - \theta)}{\lambda\sqrt{d^2 + r^2 + R^2}}\right] J_l\left(\frac{2\pi r\sqrt{R^2 + d^2 \sin^2\phi - 2Rd \sin\phi \cos(\psi_m + a_R - \theta)}}{\lambda\sqrt{d^2 + r^2 + R^2}}\right)}_{C_{m,l}}. \tag{9}
\end{aligned}$$

In Eq. (9), the l -order Bessel function is given as follows:

$$J_l(\alpha) = \frac{1}{2\pi} \int_0^{2\pi} e^{jl\tau} e^{-j\alpha \sin\tau} d\tau. \tag{10}$$

Observing Eq. (10), we can find that $e^{jl\tau} e^{-j\alpha \sin\tau}$ is the function, of which τ is the independent variable, with period 2π when l is an integer. This is the reason why the line 4 of Eq. (7) is equal to the line 5 of Eq. (7). Also, we replace some polynomials in Eq. (7) with h and $C_{m,l}$, respectively, as shown in Eq. (7) for convenient expression. In the following, we show two cases corresponding to different included angles θ and ϕ as follows:

Case A: When ϕ is equal to zero, the transmit and receive UCAs are coaxial and parallel to each other. In this case, the channel gain \tilde{h}_{ml} can be rewritten as follows:

$$\tilde{h}_{ml} = h J_l\left(\frac{2\pi r R}{\lambda\sqrt{d^2 + r^2 + R^2}}\right) e^{j(\psi_m + a_R - \frac{\pi}{2})l}. \tag{11}$$

We can find that the channel amplitude gain $|\tilde{h}_{ml}|$ only depends on the order of OAM-mode and ψ_m is independent on $|\tilde{h}_{ml}|$ when r , R , λ , and N are fixed. Thus, we can consider that the signals carried by different OAM-modes correspond to different channel amplitude gains.

Case B: When ϕ is equal to $\pi/2$, the transmit and receive UCAs are both on the transmit plane. In this case, we denote by $\theta = \alpha_R$ and we have

$$\begin{cases} B_m = \frac{2\pi r\sqrt{R^2 + d^2 - 2Rd \cos\psi_m}}{\lambda\sqrt{d^2 + r^2 + R^2}}; \\ C_{m,l} = \exp\left(\frac{j2\pi R d \cos\psi_m}{\lambda\sqrt{d^2 + r^2 + R^2}}\right) J_l(B_m). \end{cases} \tag{12}$$

Thus, the channel amplitude gain $|\tilde{h}_{ml}|$ depends on ψ_m apart from the order of OAM-mode.

The error, denoted by e_l , corresponding to the l th OAM-mode for the approximation in Eq. (9) is derived as follows:

$$e_l = \log_{10} \left[h C_{m,l} e^{j(\psi_m + a_R - \zeta_m)l} - \sum_{n=1}^N \frac{1}{\sqrt{N}} h_{mn} e^{j\varphi_n l} \right]. \tag{13}$$

Then, based on Eq. (9), we can rewrite y_m as follows:

$$\begin{aligned} y_m &= \sum_{l=\lfloor \frac{2-N}{2} \rfloor}^{\lfloor N/2 \rfloor} \tilde{h}_{ml} s_l \\ &= \sum_{l=\lfloor \frac{2-N}{2} \rfloor}^{\lfloor N/2 \rfloor} h C_{m,l} s_l e^{j\left[\frac{2\pi(m-1)}{M} + a_R - \zeta_m\right]l} + z_m, \end{aligned} \tag{14}$$

To recover the transmit signal corresponding to the l_0 th ($\lfloor (2-N)/2 \rfloor \leq l_0 \leq \lfloor N/2 \rfloor$) OAM-mode, the received signal y_m is multiplied with the item $C_{m,l_0}^{-1} \exp[-j(\psi_m + a_R - \zeta_m)l_0]$. Then, we denote by y_{m,l_0} the received signal related to l_0 at the m th array-element on the receive UCA and y_{m,l_0} can be written as follows:

$$\begin{aligned} y_{m,l_0} &= y_m C_{m,l_0}^{-1} e^{-j\left[\frac{2\pi(m-1)}{M} + a_R - \zeta_m\right]l} \\ &= \sum_{l=\lfloor \frac{2-N}{2} \rfloor}^{\lfloor N/2 \rfloor} h s_l e^{j(a_R - \zeta_m)(l-l_0)} e^{j\frac{2\pi(m-1)}{M}(l-l_0)} \\ &\quad + z_m C_{m,l_0}^{-1} e^{-j(\psi_m + a_R - \zeta_m)l_0}. \end{aligned} \tag{15}$$

Therefore, the received signal, denoted by y_{l_0} , corresponding to the l_0 th OAM-mode of the receive UCA can be derived as follows:

$$\begin{aligned}
y_{l_0} &= \sum_{m=1}^M y_{m,l_0} \\
&= \sum_{l=\lfloor \frac{2-N}{2} \rfloor, l \neq l_0}^{\lfloor N/2 \rfloor} h_{s_l} e^{j(a_R - \zeta_m)(l-l_0)} \sum_{m=1}^M e^{j\frac{2\pi(m-1)}{M}(l-l_0)} \\
&\quad + \sum_{m=1}^M h_{s_{l_0}} + \sum_{m=1}^M z_m C_{m,l_0}^{-1} e^{-j(\psi_m + a_R - \zeta_m)l_0} \\
&= M h_{s_{l_0}} + \sum_{m=1}^M z_m C_{m,l_0}^{-1} e^{-j(\psi_m + a_R - \zeta_m)l_0}. \quad (16)
\end{aligned}$$

Traversing the OAM-mode l_0 , we can obtain all the estimated transmit signals. Because z_m is the complex Gaussian variable with zero mean and variance σ_m^2 , we can derive that $\sum_{m=1}^M z_m C_{m,l_0}^{-1} e^{-j(\psi_m + a_R - \zeta_m)l_0}$ is a complex Gaussian variable with zero mean and variance $\sum_{m=1}^M C_{m,l_0}^{-2} \sigma_m^2$. Then, the spectrum efficiency, denoted by C_{OAM} , for the radio vortex wireless communications under the non-coaxial UCA transceiver scenario can be derived as follows:

$$C_{OAM} = \sum_{l=\lfloor \frac{2-N}{2} \rfloor}^{\lfloor N/2 \rfloor} \log_2 \left(1 + \frac{M^2 h^2 |s_l|^2}{\sum_{m=1}^M C_{m,l_0}^{-2} \sigma_m^2} \right). \quad (17)$$

IV. PERFORMANCE EVALUATIONS

In this section, we evaluate the performance of non-coaxial UCA transceiver based radio vortex wireless communications. First, we evaluate the approximation error corresponding to different OAM-modes. Then, we evaluate the channel amplitude gains for different OAM-modes versus the included angle θ and ϕ , respectively.

Figure 2 shows the approximation error of different OAM-modes for the non-coaxial UCA transceiver scenario, where we set $\beta = 4\pi$, $\alpha_r = \alpha_R = 0$, $\theta = \phi = 0$, and $\lambda = 0.1$ m. We can observe that when the number of array-elements is larger than 10, the corresponding error is very small and can be ignored. Therefore, \tilde{h}_{ml} is relatively very accurate when the number of array-elements is larger than 10. Also, the error mainly depends on the number of array-elements while the value of $2\pi r R / (\lambda \sqrt{d^2 + r^2} + R^2)$ has small impact on the error for different OAM-modes.

Figure 3 displays the values of $|\tilde{h}_{ml}|$ for different OAM-modes with respect to ϕ , where we set $\beta = 4\pi$, $N = M = 10$, $\lambda = 0.1$ m, $r = R = \lambda$, $d = 10\lambda$, $\alpha_r = \alpha_R = 0$, and $\theta = 0$. As shown in Fig. 3, the channel amplitude gain corresponding to OAM-mode 0 first decreases and then increases as the included angle ϕ increases. While the channel amplitude gains corresponding to other OAM-modes first increase and then decrease as the included angle ϕ increases. The channel amplitude gains corresponding to different basic angle ψ_m are almost the same.

Figure 4 depicts the values of $|\tilde{h}_{ml}|$ for different OAM-modes with respect to θ , where we set $\beta = 4\pi$, $N = M = 10$,

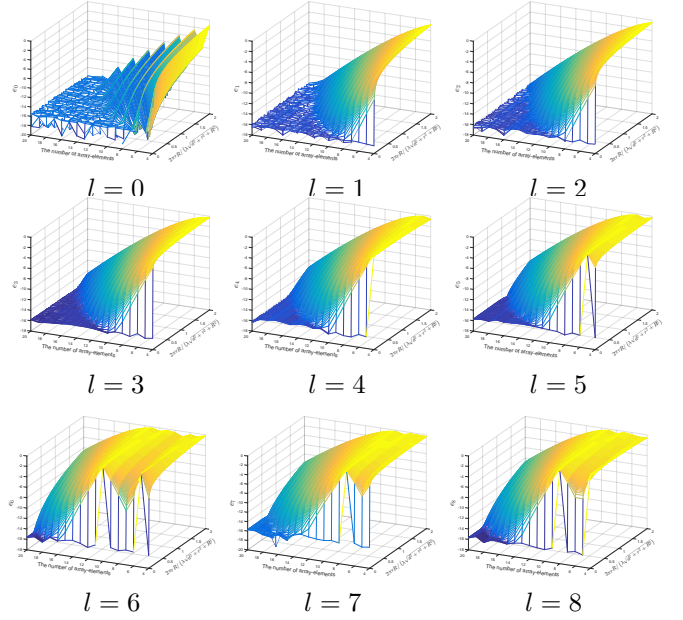


Fig. 2. Approximation error from OAM-mode 0 to OAM-mode 8.

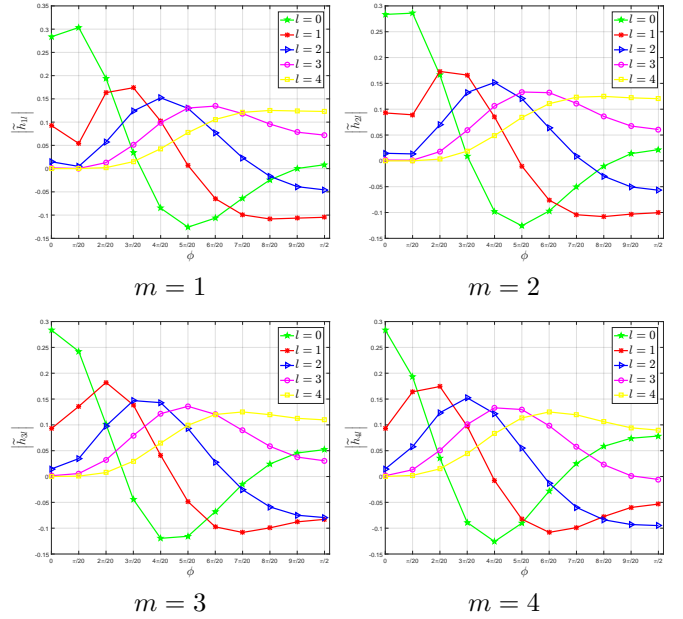


Fig. 3. $|\tilde{h}_{ml}|$ for different OAM-modes with different m .

$\lambda = 0.1$ m, $r = R = \lambda$, $d = 10\lambda$, $\alpha_r = \alpha_R = 0$, and $\phi = \pi/3$. For different ψ_m , the channel amplitude gains randomly change. Also, the dynamic range of channel amplitude gains for all the OAM-modes is small as the included angle θ increases.

Figure 5 shows the spectrum efficiency versus the included angle ϕ , where we set $\beta = 4\pi$, $N = M = 10$, $\lambda = 0.1$ m, $r = R = \lambda$, $d = 10\lambda$, $\alpha_r = \alpha_R = 0$, and $\theta = 0$. We can observe that the maximum spectrum efficiency is achieved when the included angle ϕ is approximately equal to $2\pi/5$. In some cases, the spectrum efficiency of the non-coaxial UCA transceiver is larger than that of the aligned UCA transceiver based radio vortex wireless communications. That is to say,

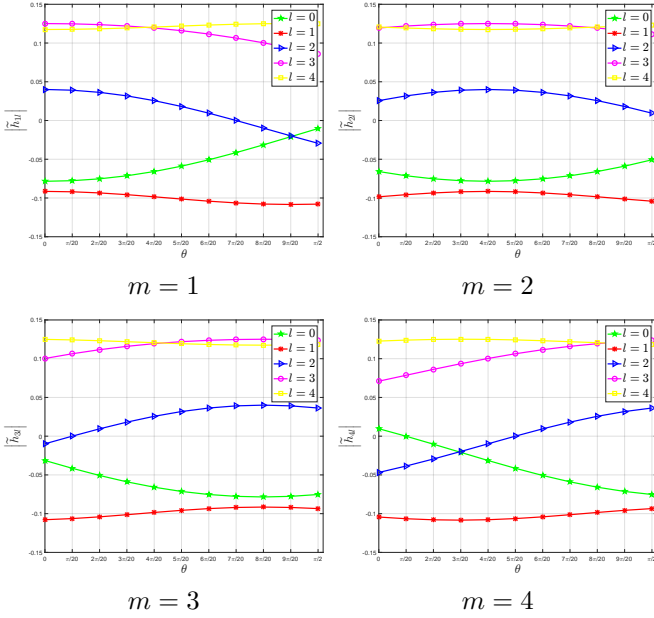


Fig. 4. $|\tilde{h}_{ml}|$ for different OAM-modes with different m .

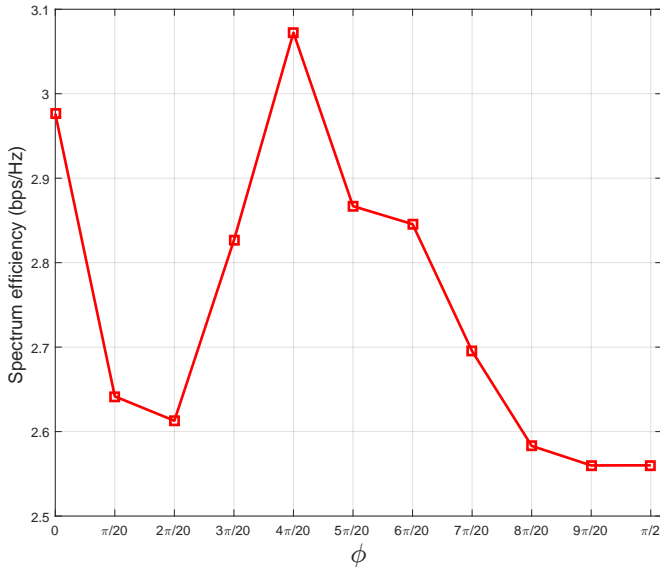


Fig. 5. The spectrum efficiency versus the included angle ϕ .

the scenario where the transmit and receive UCAs are aligned with each other is not the best scene to achieve the spectrum efficiency maximization.

V. CONCLUSIONS

We investigated the non-coaxial scenario where the transmit and receive UCAs are non-coaxial with each other. Then, we derived the channel model and developed the mode-decomposition scheme to obtain the transmit signal corresponding to each OAM-mode. Then, we discussed the impact of included angles θ and ϕ on the channel gains. The simulation results validated that in some cases the spectrum efficiency of the non-coaxial UCA transceiver is larger than

that of the aligned UCA transceiver based radio vortex wireless communications.

REFERENCES

- [1] J. G. Andrews, S. Buzzi, W. Choi, S. V. Hanly, A. Lozano, A. C. K. Soong, and J. C. Zhang, "What will 5G be?" *IEEE Journal on Selected Areas in Communications*, vol. 32, no. 6, pp. 1065–1082, June 2014.
- [2] F. Tamburini, E. Mari, A. Sponselli, F. Romanato, B. Thidé, A. Bianchini, L. Palmieri, and C. G. Someda, "Encoding many channels in the same frequency through radio vorticity: first experimental test," *New Journal of Physics*, vol. 14, no. 3, 2013.
- [3] Y. Yan, G. Xie, M. P. J. Lavery, H. Huang, N. Ahmed, C. Bao, Y. Ren, Y. Cao, L. Li, and Z. Zhao, "High-capacity millimetre-wave communications with orbital angular momentum multiplexing," *Nature Communications*, vol. 5, 2014.
- [4] K. A. Opare, Y. Kuang, J. J. Kponyo, K. S. Nwizege, and Z. Enzhan, "The degrees of freedom in wireless line-of-sight OAM multiplexing systems using a circular array of receiving antennas," in *Fifth International Conference on Advanced Computing Communication Technologies*, 2015, pp. 608–613.
- [5] Z. Zhao, Y. Yan, L. Li, G. Xie, Y. Ren, N. Ahmed, Z. Wang, C. Liu, A. J. Willner, P. Song, H. Hashemi, H. Yao, D. Macfarlane, R. Henderson, N. Ashrafi, S. Ashrafi, S. Talwar, S. Sajuyigbe, M. Tur, A. F. Molisch, and A. E. Willner, "A dual-channel 60 GHz communications link using patch antenna arrays to generate data-carrying orbital-angular-momentum beams," in *2016 IEEE International Conference on Communications (ICC)*, May 2016, pp. 1–6.
- [6] W. Zhang, S. Zheng, X. Hui, R. Dong, X. Jin, H. Chi, and X. Zhang, "Mode division multiplexing communication using microwave orbital angular momentum: An experimental study," *IEEE Transactions on Wireless Communications*, vol. 16, no. 2, pp. 1308–1318, Feb. 2017.
- [7] X. Ge, R. Zi, X. Xiong, Q. Li, and L. Wang, "Millimeter wave communications with OAM-SM scheme for future mobile networks," *IEEE Journal on Selected Areas in Communications*, vol. PP, no. 99, pp. 1–1, 2017.
- [8] Q. Zhu, T. Jiang, Y. Cao, K. Luo, and N. Zhou, "Radio vortex for future wireless broadband communications with high capacity," *IEEE Wireless Communications*, vol. 22, no. 6, pp. 98–104, Dec. 2015.
- [9] M. Cheng, L. Guo, J. Li, and Y. Zhang, "Channel capacity of the OAM-based free-space optical communication links with Bessel-Gauss beams in turbulent ocean," *IEEE Photonics Journal*, vol. 8, no. 1, pp. 1–11, Feb. 2016.
- [10] A. E. Willner, "Communication with a twist," *IEEE Spectrum*, vol. 53, no. 8, pp. 34–39, Aug. 2016.
- [11] S. M. Mohammadi, L. K. S. Daldorff, J. E. S. Bergman, R. L. Karlsson, B. Thidé, K. Forozesh, T. D. Carozzi, and B. Isham, "Orbital angular momentum in radio-a system study," *IEEE Transactions on Antennas and Propagation*, vol. 58, no. 2, pp. 565–572, Feb. 2010.
- [12] Q. Bai, A. Tennant, and B. Allen, "Experimental circular phased array for generating OAM radio beams," *Electronics Letters*, vol. 50, no. 20, pp. 1414–1415, Sep. 2014.
- [13] E. Basar, "Orbital angular momentum with index modulation," *IEEE Transactions on Wireless Communications*, vol. 17, no. 3, pp. 2029–2037, Mar. 2018.
- [14] L. Liang, W. Cheng, W. Zhang, and H. Zhang, "Mode hopping for anti-jamming in radio vortex wireless communications," to appear in *IEEE Transactions on Vehicular Technology*, pp. 1–15, 2018.
- [15] H. Jing, W. Cheng, Z. Li, and H. Zhang, "Concentric UCAs based low-order radio vortex wireless communications with co-mode interference (invited paper)," in *2017 IEEE/CIC International Conference on Communications in China (ICCC)*, Oct. 2017, pp. 1–6.
- [16] W. Cheng, W. Zhang, H. Jing, S. Gao, and H. Zhang, "Orbital angular momentum for wireless communications," to appear in *IEEE Wireless Communications Magazine*, pp. 1–15, 2018.
- [17] O. Edfors and A. J. Johansson, "Is orbital angular momentum (OAM) based radio communication an unexploited area?," *IEEE Transactions on Antennas and Propagation*, vol. 60, no. 2, pp. 1126–1131, 2012.